Klas Lindfors, Arri Priimagi, Tero Setälä, Andriy Shevchenko, Ari T. Friberg, and Matti Kaivola. 2007. Local polarization of tightly focused unpolarized light. Nature Photonics, volume 1, number 4, pages 228-231.

Local polarization of tightly focused unpolarized light

KLAS LINDFORS[1]*, ARRI PRIIMAGI[1], TERO SETÄLÄ[1], ANDRIY SHEVCHENKO[1], ARI T. FRIBERG[2] AND MATTI KAIVOLA[1]

[1]Helsinki University of Technology (TKK), Department of Engineering Physics and Mathematics and Center for New Materials, PO Box 3500, FI-02015 TKK, Finland
[2]Royal Institute of Technology (KTH), School of Information and Communication Technology, Electrum 229, SE-164 40 Kista, Sweden
*e-mail: klas.lindfors@tkk.fi

Published online: 2 April 2007; doi:10.1038/nphoton.2007.30

The polarization of light is important in a great variety of optical phenomena, ranging from transmission, reflection and scattering to polarimetric imaging of scenes and quantum-mechanical selection rules of atomic and molecular transitions. Among some less-well-known phenomena that illustrate the vectorial nature of light are the Pancharatnam[1] (or geometric[2]) phase, singularities in the polarization pattern of clear sky[3] and polarization of microwave background radiation[4]. Here, we examine the partial polarization of focused light. We experimentally demonstrate a rather surprising phenomenon, where the focusing of unpolarized light results in rings of full polarization in the focal plane of the focusing optics. The polarization rings are imaged with a resolution of <100 nm by probing the focal region using a gold nanoparticle.

Recent advances in nano-optics have made the polarization properties of tightly focused light a subject of intense research[5–12]. The state of polarization in the focal region of an imaging system with a high numerical aperture (NA) exhibits a multitude of features related to the three-dimensional character of the electromagnetic field. For example, it has been shown that the shape of the focal spot can be controlled by using azimuthally or radially polarized illumination[9] and that the area of the focus may be extremely small when radial polarization is used[10]. In optical microscopy, polarized light has been used to determine the three-dimensional orientation of individual molecules[6–8]. The polarization of light has also been applied to the orientation of nanoscale particles in optical tweezers for nanostructuring applications[5].

Research on the polarization properties of tightly focused optical fields has so far concentrated predominantly on fully polarized light, and partially polarized waves have received less attention. We recently studied theoretically high-NA focusing of partially polarized light and showed that an unpolarized incident beam of light locally becomes fully polarized in the focal region[12]. Here we report on the experimental observation of this effect by mapping the distribution of the degree of polarization in the focal plane of a high-NA microscope objective.

The degree of polarization at point $\mathbf{r}$ and frequency ω, $P_{3D}(\mathbf{r}, \omega)$, of a random wave field that has three vector components can be written in terms of the coherence matrix $\Phi_{3D}(\mathbf{r}, \omega)$ (refs 13 and 14) as

$$P_{3D}^2(\mathbf{r}, \omega) = \frac{3}{2}\left\{\frac{\mathrm{Tr}\Phi_{3D}^2(\mathbf{r}, \omega)}{\mathrm{Tr}^2\Phi_{3D}(\mathbf{r}, \omega)} - \frac{1}{3}\right\} \qquad (1)$$

where 'Tr' denotes the trace operation[15–17]. A similar expression for the degree of polarization of planar (two-dimensional) fields is given by

$$P_{2D}^2(\mathbf{r}, \omega) = 1 - \frac{4\det[\Phi_{2D}(\mathbf{r}, \omega)]}{\mathrm{Tr}^2\Phi_{2D}(\mathbf{r}, \omega)} = 2\left\{\frac{\mathrm{Tr}\Phi_{2D}^2(\mathbf{r}, \omega)}{\mathrm{Tr}^2\Phi_{2D}(\mathbf{r}, \omega)} - \frac{1}{2}\right\} \qquad (2)$$

where 'det' stands for the determinant of the matrix[13,14]. The degree of polarization given by equation (1), or equation (2) in two dimensions, is determined by the correlations between the orthogonal electric-field components. It is bounded by 0 and 1, which correspond to unpolarized and fully polarized fields, respectively.

The focusing of partially polarized light can be modelled by first calculating the electric field in the focal region for one realization of the incident fluctuating electromagnetic wave and then averaging over the appropriate ensemble[12,13]. In this way, we obtain the distribution of the three-dimensional degree of polarization of a focused unpolarized plane wave, as shown in Fig. 1. The appearance of the polarized rings surrounding the focus is explained by the fact that at the points falling on these rings, all three electric-field components are proportional to the same combination of the two incident-field components, that is to the same random function[12,18]. This effect is present in focusing not only of plane waves but also, for instance, of gaussian beams.

To image the polarization distribution of a tightly focused optical field we use a gold nanoparticle as a probe. Gold nanoparticles have previously been successfully demonstrated in use as miniature probes in near-field microscopy to map intensity distributions[19]. For a spherical nanoparticle with a radius much smaller than the wavelength of light, the optically induced dipole moment $\mathbf{p}$ is directly proportional to the local electric field $\mathbf{E}$ (ref. 20). By analysing the scattered far-field radiation as the particle is scanned, the polarization properties of the light are mapped. The dipole induced on the particle radiates an outgoing wave, which is collimated by a lens, so that a planar-wave field, $\mathbf{E}'$, results. This two-dimensional field at the point $\mathbf{r}'$ is related to the three-dimensional field at the point $\mathbf{r}$ of the particle in the focal region of the lens by a transformation $\mathbf{E}'(\mathbf{r}', \mathbf{r}) = A(\mathbf{r}', \mathbf{r})\mathbf{E}(\mathbf{r})$, where $A(\mathbf{r}', \mathbf{r})$ is a real-valued 2×3 geometry-dependent matrix[21]. The coherence matrix of the observed field is now written as

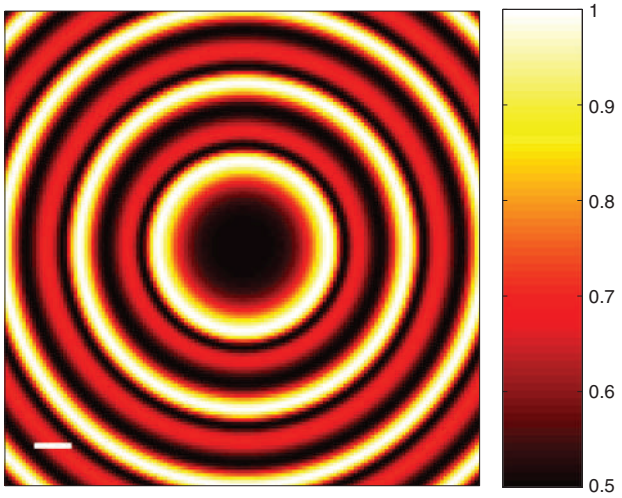

Figure 1 Distribution of P_{3D} in the focal plane of a high-NA lens. The incident light (wavelength 532 nm) is an unpolarized plane wave ($P_{2D} = 0$; note that in the three-dimensional representation such waves have $P_{3D} = 0.5$; refs 16 and 17). The NA of the lens is 1.3 and the refractive index in the focal region is 1.5. The scale bar represents 100 nm. The coloured scale represents P_{3D}.

$\Phi_{2D}(\mathbf{r}', \mathbf{r}, \omega) = A(\mathbf{r}', \mathbf{r})\Phi_{3D}(\mathbf{r}, \omega)A^{T}(\mathbf{r}', \mathbf{r})$ where $A^{T}(\mathbf{r}', \mathbf{r})$ is the transpose of $A(\mathbf{r}', \mathbf{r})$.

In our experiment, a beam of light with tunable polarization properties is produced by combining two uncorrelated, orthogonally linearly polarized laser beams ($\lambda = 532$ nm). The beams are passed through a single-mode optical fibre to make them fully co-propagating. By varying the ratio γ of the intensities of the two beams, the degree of polarization of the resulting beam, $P_{2D} = |1 - \gamma|/(1 + \gamma)$, can be changed[13,14]. The light emerging from the fibre is collimated and directed into an inverted microscope, in which it is focused with a high-NA microscope objective (NA = 1.3). The distribution of the polarization in the focal region is probed with a single 80-nm-diameter gold nanoparticle as illustrated in Fig. 2.

Our measurement technique is based on the correspondence between the degrees of polarization of the probed and scattered fields. The measurement yields Φ_{2D} for the scattered field and, using equation (2), we obtain P_{2D} as a function of the position, $\mathbf{r}$, of the nanoparticle in the focal plane. Figure 3 shows the measurement result for the case of unpolarized incident light. As predicted, we observe a thin ring of polarized light around the focus. Within the area enclosed by the ring, the degree of polarization is approximately zero, but on the ring it attains markedly high values. A slight aberration of the ring in its upper part is presumably caused by wavefront distortions of the light at the entrance of the objective. The inset in Fig. 3 shows the theoretically calculated distribution for the measured P_{2D}. The calculation was performed by using the formalism of vector-wave focusing with high-NA objectives to obtain $\mathbf{E}(\mathbf{r})$ (ref. 12), from which $\Phi_{3D}(\mathbf{r}, \omega)$, $\Phi_{2D}(\mathbf{r}', \mathbf{r}, \omega)$ and finally P_{2D} follow. The imaging geometry is included in $A(\mathbf{r}', \mathbf{r})$. The experimental observation shows good agreement with the calculated profile, and it is fully consistent with the P_{3D} distribution shown in Fig. 1.

When the degree of polarization of the incident field is increased, the scattered light as a whole becomes more polarized, as seen in Fig. 4. The essential experimental observations agree with the theoretical predictions. A rather surprising feature is the appearance of a thin ring of (almost)

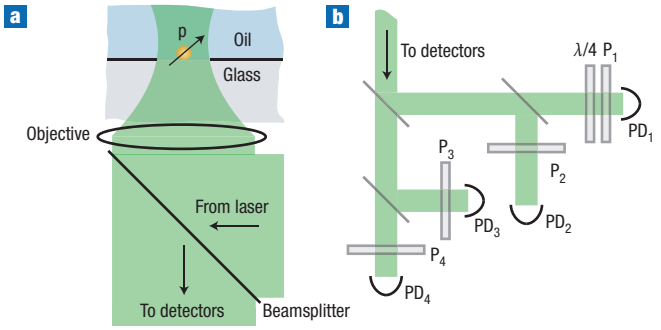

Figure 2 Experimental set-up for mapping the degree of polarization. **a**, Schematic of the sample geometry. Gold nanoparticles are spin-coated on a glass substrate (surface density less than 0.1 μm^{-2}). A drop of immersion oil (refractive index 1.5) is added to the sample in order to suppress the strong reflection from the cover-glass–air interface. The sample, mounted in an inverted microscope, is raster-scanned in the focal plane using a piezo-electric positioning system. The light backscattered by a single nanoparticle as it passes through the focus is collected by the focusing objective, collimated and directed to a polarization analyser. **b**, Schematic of the polarization analyser. The degree of polarization of the scattered light is determined by performing four intensity measurements to obtain the elements of the 2×2 coherence matrix. The scattered light is studied with an analyser in which light is split into four arms to measure three linearly polarized and one circularly polarized component (P_i are polarizers, $\lambda/4$ is a quarter-wave plate, and PD_i are photodetectors). The method is described in more detail in Section 6.2 of ref. 13. Note that the unavoidable slight polarization dependencies of the optical elements in the set-up are thoroughly taken into account in the measurements.

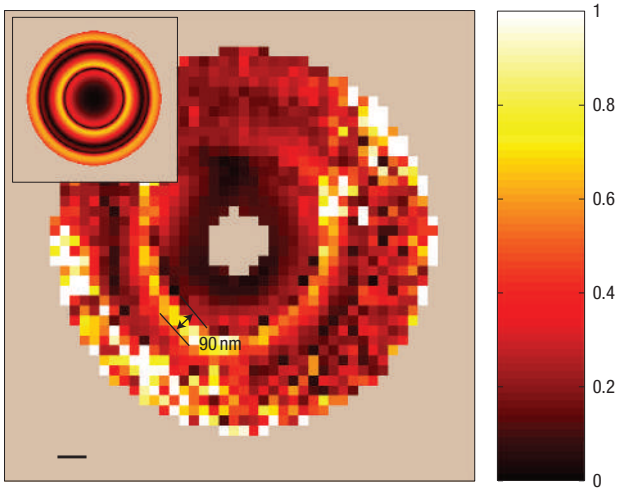

Figure 3 Polarization by focusing. The measured degree of polarization P_{2D} of the light scattered by a single nanoparticle as a function of its position in the focal plane of the microscope objective. The incident field is unpolarized. The inset shows the theoretical prediction for the measured signal. The measured NA of the focused beam is approximately 1.14. The scale bar is 100 nm. At the centre of the focus, the detectors are saturated due to the high intensity, and far away from the focus, the intensity is too low to provide information about the polarization distribution. Hence, these areas are not included in the data. The coloured scale represents P_{2D}.

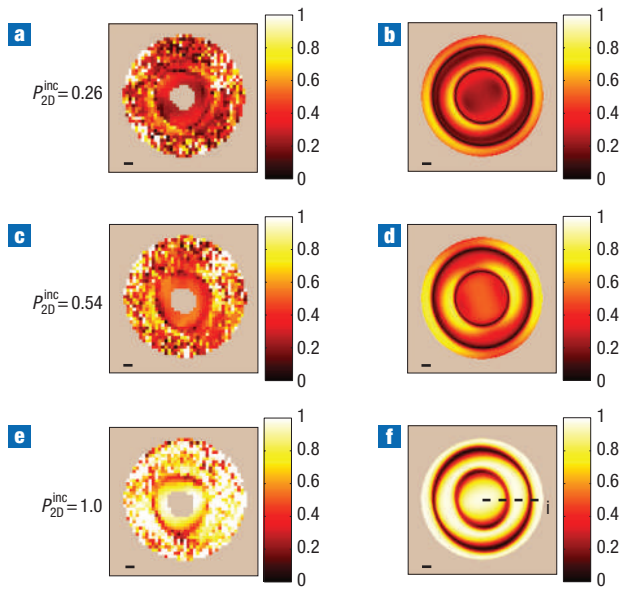

Figure 4 Measured P_{2D} for different values of the degree of polarization of the incident beam P_{2D}^{inc}. **a**,**c**,**e**, Experimental observations. **b**,**d**,**f**, Corresponding theoretical predictions. In **a** and **b** $P_{2D}^{inc} = 0.26$; in **c** and **d**, $P_{2D}^{inc} = 0.54$, and in **e** and **f**, $P_{2D}^{inc} = 1.0$. All scale bars are 100 nm. All the coloured scales represent P_{2D}.

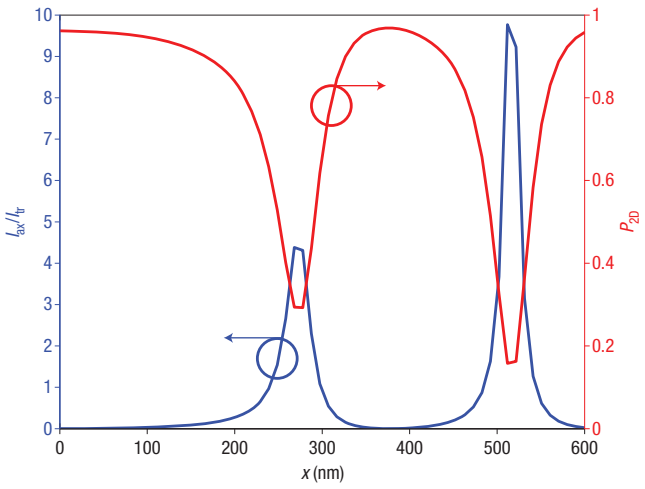

Figure 5 Influence of the axial electric-field component on P_{2D}. The theoretically calculated ratio of the intensities of the electric-field components along I_{ax} and perpendicular I_{tr} to the optical axis (blue curve) and the degree of polarization P_{2D} (red curve) are shown for the cut (i) of Fig. 4f.

unpolarized light with a radius of about 250 nm. This ring is present even in the case of fully polarized incident light in both the measured and the calculated polarization profiles. In fact, the low measured values on the ring just trace the points where the electric field is mainly polarized along the optical axis. The polarization distribution of the light scattered by the nanoparticle from such points is circularly symmetric in the input plane of the objective. Consequently, the degree of polarization measured with the analyser drops in value. This is confirmed in Fig. 5, in which the calculated degree of polarization along the cross section (i) in Fig. 4f is shown together with the ratio of the intensities of the electric-field components along and perpendicular to the optical axis. When the nanoparticle is located close to points of such longitudinally polarized light, the polarization state of the scattered field at the entrance of the objective is distinctly non-uniform, which affects the measurement. Mathematically, the rings of lowered degree of polarization come from mixing of coherence matrix elements by the matrix $A(\mathbf{r}', \mathbf{r})$ when going from the focal region to the far field.

To summarize, we have experimentally studied the polarization properties of a tightly focused optical field and observed incident two-dimensional unpolarized light become locally polarized in the focal region. The results also demonstrate that the polarization state may change considerably on a scale much shorter than the wavelength.

Knowledge of the polarization properties of tightly focused light is of particular interest for researchers working in the field of nano-optics, because the coupling of light to nanostructured matter is essentially always carried out through high-NA focusing. The polarization-mapping technique introduced in this work can be applied to obtain high-resolution polarization distributions in both propagating and evanescent optical fields. This technique is quite general, and can be further developed and modified in order to match specific experimental requirements. For example, the complete three-dimensional polarization picture can be obtained by performing the measurements in three mutually perpendicular observation directions. Our results are expected to attract further interest to subwavelength-scale statistical features of fluctuating electromagnetic fields, which can bring about novel approaches to nanoscale-resolution imaging based purely on optical fields.

Received 15 December 2006; accepted 21 February 2007; published 2 April 2007.

References

1. Pancharatnam, S. Generalized theory of interference and its applications. Part I. Coherent pencils. *Proc. Ind. Acad. Sci. A.* **44,** 247–262 (1956).
2. Hariharan, P. The geometric phase. In *Prog. Opt.*, vol. 48 (ed. Wolf, E.) 149–201 (Elsevier, Amsterdam, The Netherlands, 2005).
3. Berry, M. V., Dennis, M. R. & Lee R. L. Jr. Polarization singularities in the clear sky. *New J. Phys.* **6,** 162 (2004).
4. Kovac, J. M. *et al.* Detection of polarization in the cosmic microwave background using DASI. *Nature* **420,** 772–787 (2002).
5. Friese, M. E. J., Nieminen, T. A., Heckenberg, N. R. & Rubinsztein-Dunlop, H. Optical alignment and spinning of laser-trapped microscopic particles. *Nature* **394,** 348–350 (1998).
6. Empedocles, S. A., Neuhauser, R. & Bawendi, M. G. Three-dimensional orientation measurements of symmetric single chromophores using polarization microscopy. *Nature* **399,** 126–130 (1999).
7. Sick, B., Hecht, B. & Novotny, L. Orientational imaging of single molecules by annular illumination. *Phys. Rev. Lett.* **85,** 4482–4485 (2000).
8. Novotny, L., Beversluis, M. R., Youngworth, K. S. & Brown, T. G. Longitudinal field modes probed by single molecules. *Phys. Rev. Lett.* **86,** 5251–5254 (2001).
9. Youngworth, K. S. & Brown, T. G. Focusing of high numerical aperture cylindrical-vector beams. *Opt. Express* **7,** 77–87 (2000).
10. Dorn, R., Quabis, S. & Leuchs, G. Sharper focus for a radially polarized light beam. *Phys. Rev. Lett.* **91,** 233901 (2003).
11. Ellis, J. & Dogariu, A. Optical polarimetry of random fields. *Phys. Rev. Lett.* **95,** 203905 (2005).
12. Lindfors, K., Setälä, T., Kaivola, M. & Friberg, A. T. Degree of polarization in tightly focused optical fields. *J. Opt. Soc. Am. A.* **22,** 561–568 (2005).
13. Mandel, L. & Wolf, E. *Optical Coherence and Quantum Optics* (Cambridge Univ. Press, Cambridge, 1995).
14. Brosseau, C. *Fundamentals of Polarized Light. A Statistical Optics Approach* (Wiley, New York, 1998).
15. Setälä, T., Kaivola, M. & Friberg, A. T. Degree of polarization in near fields of thermal sources: effects of surface waves. *Phys. Rev. Lett.* **88,** 123902 (2002).
16. Setälä, T., Shevchenko, A., Kaivola, M. & Friberg, A. T. Degree of polarization for optical near fields. *Phys. Rev. E* **66,** 016615 (2002).
17. Brosseau, C. & Dogariu, A. Symmetry properties and polarization descriptors for an arbitrary electromagnetic wavefield. In *Prog. Opt.*, vol. 49 (ed. Wolf, E.) 315–380 (Elsevier, Amsterdam, The Netherlands, 2006).
18. Ellis, J., Dogariu, A., Ponomarenko, S. & Wolf, E. Correlation matrix of a completely polarized, statistically stationary electromagnetic field. *Opt. Lett.* **29,** 1536–1538 (2004).

19. Kalkbrenner, T., Ramstein, M., Mlynek, J. & Sandoghdar, V. A single gold particle as a probe for apertureless scanning near-field optical microscopy. *J. Microsc.* **202,** 72–76 (2001).
20. Bohren, C. F. & Huffman, D. R. *Absorption and Scattering of Light by Small Particles* (Wiley-Interscience, New York, 1983).
21. Wilson, T., Juškaitis, R. & Higdon, P. The imaging of dielectric point scatterers in conventional and confocal polarisation microscopes. *Opt. Commun.* **141,** 298–313 (1997).

Acknowledgements

The authors from TKK acknowledge financial support from the Academy of Finland, project numbers 201293 and 118074, and A.T.F. acknowledges the support of the Swedish Foundation for Strategic Research. J. Pekola and O. Hahtela are thanked for loans of equipment.
Correspondence and requests for materials should be addressed to K.L.

Competing financial interests

The authors declare that they have no competing financial interests.